A Contactless Method for Determining the Carrier Mobility Sum in Silicon Wafers

Fiacre E. Rougieux, Peiting Zheng, Matthieu Thiboust, Jason Tan, Nicholas E. Grant, Daniel H. Macdonald, and Andres Cuevas

***Abstract*—In this paper, we present a new method to determine the simultaneous injection and temperature dependence of the sum of the majority and minority carrier mobilities in silicon wafers. The technique is based on combining transient and quasi-steady-state photoconductance measurements. It does not require a full device structure or contacting but only adequate surface passivation. The mobility dependence on both carrier injection level and temperature, as measured on several test samples, is discussed and compared with well-known mobility models. The potential of this method to measure the impact of dopant concentration, compensation ratio, injection level, and temperature on the mobility is demonstrated.**

***Index Terms*—Charge carrier mobility, photoconductance, silicon, solar cells.**

I. Introduction

THE carrier mobility is a key parameter in determining the performance of silicon solar cells. It is well known that the mobility decreases with both carrier injection level [1], [2] and sample temperature [3]. Since solar cells often operate under a wide range of injection levels and temperatures, it is, thus, fundamental to determine the impact of those parameters on the carrier mobility. Numerous techniques have been used to measure the mobility, and the impact of dopant concentration and temperature is well known in standard, non-compensated crystalline silicon. Nevertheless, data on the impact of injection or the simultaneous impact of carrier injection and temperature on the carrier mobility are scarce. Furthermore, the effect of dopant compensation on carrier mobilities, especially for minority carriers, remains unclear [4]–[6].

Dannhauser and Krausse used a combination of infrared radiation and voltage measurements across a pin diode to extract the injection dependence of the mobility sum [1], [2]. Similarly, Neuhaus *et al*. used a combination of quasisteady-state photoconductance (QSSPC) and quasisteady-state open-circuit-voltage measurements on a solar cell to determine the injection dependence of the mobility sum [7]. However, both of these methods require a complicated structure and need contacting. In this paper, we propose and demonstrate a new technique based on contactless photoconductance measurements.

Manuscript received July 11, 2011; revised November 2, 2011; accepted November 4, 2011. Date of publication December 5, 2011; date of current version January 30, 2012. This work was supported by the Australian Research Council.

The authors are with the Research School of Engineering, College of Engineering and Computer Science, The Australian National University, Canberra, A.C.T. 0200, Australia (e-mail: fiacre.rougieux@anu.edu.au; u4433025@anu.edu.au; matthieu_thiboust@yahoo.fr; jason.tan@anu.edu.au; nicholas.grant@anu.edu.au; daniel.macdonald@anu.edu.au; andres.cuevas@anu.edu.au).

Color versions of one or more of the figures in this paper are available online at http://ieeexplore.ieee.org.

Digital Object Identifier 10.1109/JPHOTOV.2011.2175705

II. Theoretical Principles

Two common measurement methods are used to determine effective carrier lifetimes in silicon. The first one, which is referred to as transient photoconductance decay (PCD) measures the rate at which carriers recombine after a short excitation pulse. The lifetime is extracted via

$$\tau_{\mathrm{PCD}} = -\frac{\Delta n}{(d\Delta n/dt)} \tag{1}$$

where τ_{PCD} is the transient lifetime, Δn is the excess carrier density, and $d\Delta n/dt$ is the variation of excess carrier with time. The second method, i.e., QSSPC, measures the balance between generation and recombination when a quasisteady-state illumination is maintained. The generalized lifetime [8] is then extracted as

$$\tau_{\mathrm{QSSPC}} = \frac{\Delta n}{G_{\mathrm{QSSPC}} - (d\Delta n/dt)} \tag{2}$$

where τ_{QSSPC} is the quasistatic lifetime, and $\mathrm{G_{QSSPC}}$ is the generation within the sample. At this point, it is interesting to note that the transient technique requires samples with lifetimes significantly longer than the characteristic decay of the excitation flash. In our case, this corresponds to lifetimes higher than 100 μs. If a light source with shorter cutoff times is used, this value can be reduced, and lower lifetime samples can be measured with the PCD technique.

However, it should also be kept in mind that samples with low effective lifetimes, whether because of either surface or bulk recombination, can easily result in nonuniform carrier profiles throughout the wafer thickness. In such cases, the transient lifetime and the quasistatic lifetime are not expected to be equal [9], [10]. The method that is described here can only be applied when these two lifetimes are equivalent, which will be the case when the carrier profiles remain approximately uniform during the transient decay. This in turn will be true when the minority carrier diffusion length is greater than the sample thickness, and the initial rapid transient modes are excluded from the analysis. These conditions were satisfied for our samples.

Assuming that at the same excess conductance the transient lifetime τ_{PCD} and quasisteady-state lifetime τ_{QSSPC} are indeed equal, we have

$$\tau_{\mathrm{PCD}}\left(\Delta\sigma\right) = \tau_{\mathrm{QSSPC}}\left(\Delta\sigma\right) \tag{3}$$

$$\frac{d\Delta n_{\mathrm{PCD}}}{dt}(\Delta\sigma) = \frac{d\Delta n_{\mathrm{QSSPC}}}{dt}(\Delta\sigma) - G_{\mathrm{QSSPC}}(\Delta\sigma). \quad (4)$$

The excess carrier concentration Δn is related to the excess conductance $\Delta\sigma$ by the relation

$$\Delta n = \frac{\Delta\sigma}{qW(\mu_n + \mu_p)} \quad (5)$$

where μ_n and μ_p are the electron and hole mobility, respectively, q is the electronic charge, and W is the sample thickness. By manipulating these expressions, one obtains

$$\begin{aligned}&(qW(G_{\mathrm{QSSPC}})(\Delta\sigma))(\mu_n+\mu_p)^2 \\ &\quad + \left(\frac{d\Delta\sigma_{\mathrm{PCD}}}{dt} - \frac{d\Delta\sigma_{\mathrm{QSSPC}}}{dt}\right)(\Delta\sigma)(\mu_n+\mu_p) \\ &\quad + \left(\Delta\sigma_{\mathrm{QSSPC}}.\frac{d(\mu_n+\mu_p)_{\mathrm{QSSPC}}}{dt}\right)(\Delta\sigma) \\ &\quad - \left(\Delta\sigma_{\mathrm{PCD}}.\frac{d(\mu_n+\mu_p)_{\mathrm{PCD}}}{dt}\right)(\Delta\sigma) = 0. \quad (6)\end{aligned}$$

However, as the mobility varies only very slightly compared with the other time-dependent quantities, one can neglect the final two terms on the left-hand side. One can, thus, easily extract the mobility sum $(\mu_n + \mu_p)$ as

$$(\mu_n+\mu_p) = \frac{1}{qWG_{\mathrm{QSSPC}}}\left(\frac{d\Delta\sigma_{\mathrm{QSSPC}}}{dt} - \frac{d\Delta\sigma_{\mathrm{PCD}}}{dt}\right) \quad (7)$$

where q is the electronic charge, W is the sample thickness, and $d\Delta\sigma_{\mathrm{QSSPC}}/dt$ and $d\Delta\sigma_{\mathrm{PCD}}/dt$ are the variation of conductance with time for the quasisteady state and transient excitation, respectively. Fig. 1 shows the dependence of the aforementioned quantities with excess conductance. By comparing the excess conductance variation with time [see Fig. 1(a)] and the generation [see Fig. 1(b)] for a transient and quasisteady-state measurement, one can thus obtain the excess conductance-dependent mobility sum [see Fig. 1(c)]. This mobility sum is in turn used to compute the excess carrier density from the excess conductance using (5).

We estimated an uncertainty of $\pm$ 3% in the measurement of the generation G_{QSSPC} and an uncertainty of $\pm$ 5% in the measurement of the conductance $\Delta\sigma$ [11]. In Fig. 1(c), at an excess conductance of $\Delta\sigma = 7 \times 10^{-2}\ \Omega^{-1}\cdot\mathrm{cm}^{-1}$, the error in the calculated mobility sum is 9.9%. However, at a lower excess conductance of $\Delta\sigma = 1 \times 10^{-2}\ \Omega^{-1}\cdot\mathrm{cm}^{-1}$, the error increases to 11.4%. We found that the mobility sum can be obtained with a 9–14% above this excess conductance.

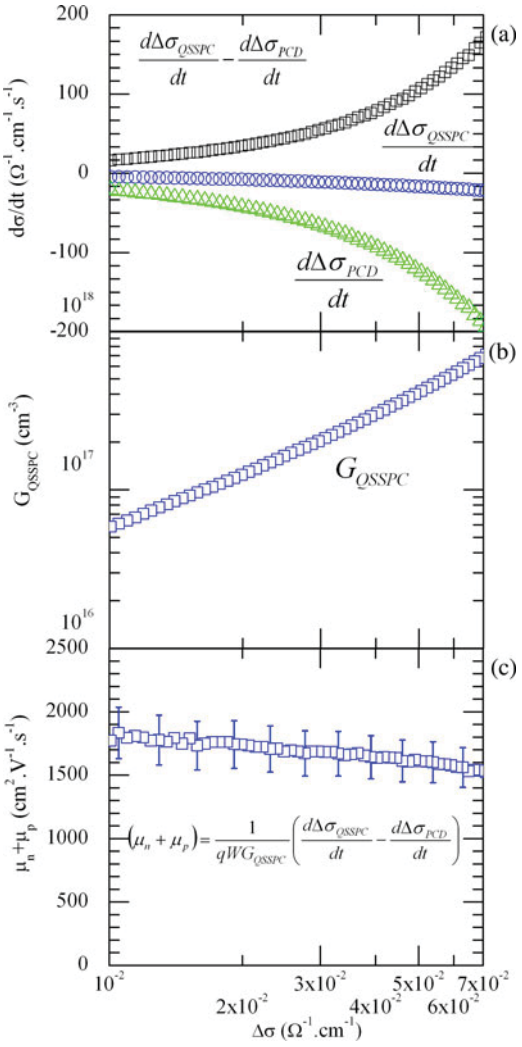

Fig. 1. Excess conductance dependence of the time derivative of (a) the conductance, (b) generation, and (c) the resulting mobility sum in a 1 Ω·cm n-type silicon wafer.

III. Experimental Methods

A. Transient and Quasi-Steady-State Photoconductance Measurements

The new method is based on combining QSSPC [12] and transient PCD lifetime measurements. The carrier lifetimes that were measured with such methods rely on a calibrated coil to measure the excess conductance and a reference solar cell to measure the generation rate. To obtain a more uniform carrier generation profile, an infrared filter was used to cutoff wavelengths below 800 nm. In order to measure the simultaneous temperature and injection dependence of the mobility, we used a purpose built, temperature-controlled inductive coil photoconductance instrument from Sinton Instruments [13].

The samples were prepared by damage etching and RCA cleaning, which was followed by surface passivation at 400 °C with plasma-enhanced chemical vapor-deposited silicon nitride films.

As described previously, the data analysis requires the calculation of a derivative with respect to time of the excess conductance signal. Therefore, any noise in this signal will be dramatically amplified. To reduce noise, each transient and QSSPC measurement is thus averaged 60 times before being processed. Another important point is that the QSSPC technique is sensitive to the optical properties of the sample. The QSSPC measurement is usually corrected using an optical scaling factor f_s [14].

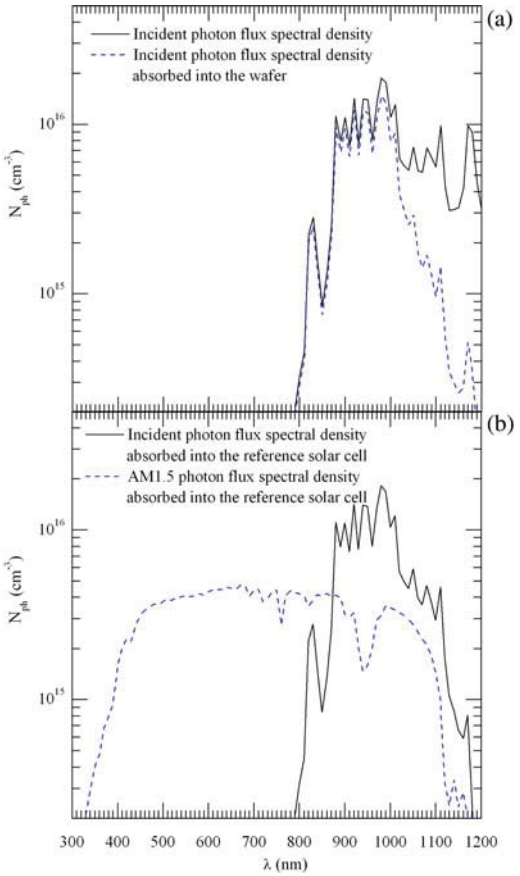

Fig. 2. (a) Incident photon flux spectral density and photon flux spectral density absorbed in the sample. The ratio of those two quantities will determine the effective optical transmission [11]. (b) Incident photon flux spectral density absorbed into the reference solar cell and AM1.5 photon flux spectral density absorbed into the reference solar cell. The ratio of those two quantities will determine the spectral correction factor [11].

B. Determination of the Optical Factor

The optical factor can be obtained through self-calibration of the generation in an intermediate photoconductance regime [14] or through direct comparison of the optical properties of the sample and the reference cell that was used in the lifetime tester [15], [16].

The optical factor will influence the generation within the sample. If inaccurate, the whole mobility curve will shift up or down (7); it is thus extremely important to accurately determine the optical factor.

We measured the absorption in our wafer using a Perkin–Elmer spectrophotometer. Using the measured absorption, we determined the effective optical transmission as described in [16]. Fig. 2(a) shows the incident photon flux density as a function of wavelength. Also shown is the photon flux spectral density that is absorbed into the wafer. Using the ratio of (integrated photon density absorbed into the wafer)/(integrated incident photon density), we then determine the effective optical transmission [16].

The standard calibration of the reference solar cell is performed under AM1.5 conditions. However, the spectrum of the flash is significantly different than AM1.5: even more so when

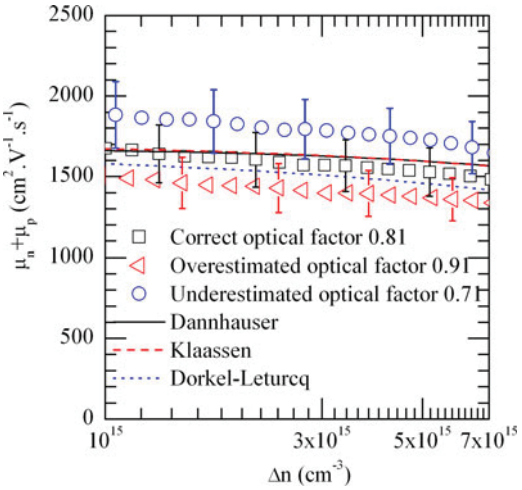

Fig. 3. Measured injection dependence of the mobility sum and impact of the optical factor. An overestimation of the optical factor leads to an underestimation of the mobility sum.

filtered by an infrared filter [see Fig. 2(b)]. We thus calculate a spectral correction factor to account for the spectral difference between the AM1.5 spectrum and the filtered flash spectrum as proposed in [15] using the ratio of (integrated AM1.5 photon flux density that is absorbed into the reference solar cell)/(integrated flash photon flux density that is absorbed into the reference solar cell).

Finally, we combined the effective optical transmission and the spectral correction factor to determine the optical factor [15]. In our wafers that were coated with SiN, when using an infrared filter (800 nm), we found the optical factor to lie between 0.68 and 0.9 depending mainly on the thickness of the wafer that was used and the variation in the optical properties of the antireflection coating. Fig. 3 shows the influence of the optical factor on the mobility sum. Overestimating the optical factor leads to an underestimation of the mobility sum. The method, thus, greatly relies on a precise measurement of the optical factor in order to give accurate results.

IV. Results and Discussion

A. Accuracy of the Method

To demonstrate the accuracy of the method, the mobility sum was measured in samples with similar resistivities (100–1000 Ω·cm, 0.90 Ω·cm p-type) to the sample that was used by Dannhauser (1000–3000 Ω·cm p-type) [1] and the samples that were used by Neuhaus *et al.* (0.96 Ω·cm p-type) [7]. Fig. 4 shows the resulting mobility sum and the mobility models of Dannhauser–Krausse [1], [2], Klaassen [17], [18], and Dorkel–Leturcq [19]. Within error, the measured mobility and the data from Dannhauser [see Fig. 4(a)] and Neuhaus [see Fig. 4(b)] are in relatively good agreement. This confirms that the method is accurate in this excess carrier density range. The measured data also fit very well with the models of Dannhauser–Krausse and Klaassen. The model of Dorkel–Leturcq lies a little below the measured values at higher doping densities.

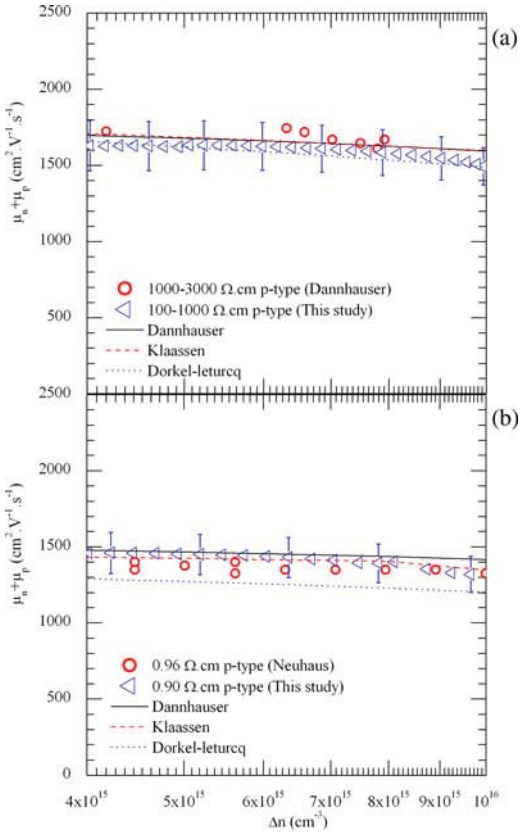

Fig. 4. (a) Measured injection dependence of the mobility sum in a 100–1000 Ω·cm p-type silicon wafer. Also shown are the data of Dannhauser. (b) Measured injection dependence of the mobility sum in a 0.90 Ω·cm p-type silicon wafer. The data of Neuhaus are also shown. The lines are from the models of Dorkel–Leturcq, Klaassen, and Dannhauser.

Although the measured mobility sum aligns with the models relatively well at medium injection (above 1×10^{15} cm^{-3}), at lower injection, the measurement becomes quite inaccurate. This is because of the fact that the derivatives of the quasi-static and transient conductances become very similar; thus, the uncertainty in their difference becomes greater, as mentioned previously. Therefore, a small uncertainty in one or the other leads to great uncertainties in the calculated mobility (7). Moreover, the signal/noise ratio of the photoconductance signal itself decreases at low injection, leading to greater errors in the measured mobility. In addition, the mobility is also inaccurate at high injection because of the effective lifetime being reduced (Auger recombination), leading to difficulties in making accurate transient measurements, and potentially causing nonuniform carrier profiles.

B. Measuring the Influence of Dopant Density

Fig. 5 shows the doping dependence of the mobility sum in n-type silicon. The lines represent the models of Dorkel–Leturcq and Klaassen. We clearly see the increasing influence of ionized impurity scattering on the mobility as the doping increases. This mobility is measured at an injection level of 5×10^{15} cm^{-3}. Within error, we obtain an excellent agreement with the mobility models.

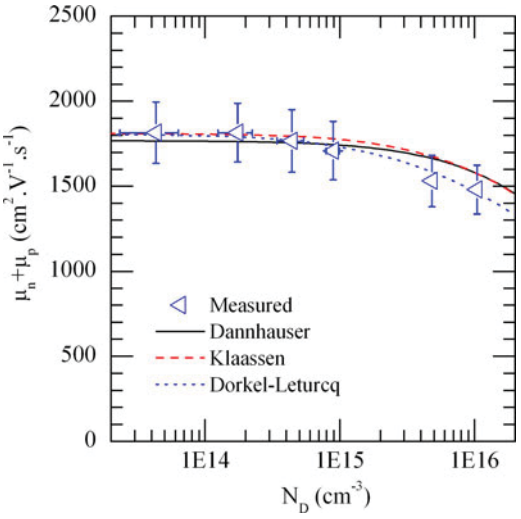

Fig. 5. Doping dependence of the mobility sum in n-type silicon. The lines represent the models of Dorkel–Leturcq and Klaassen.

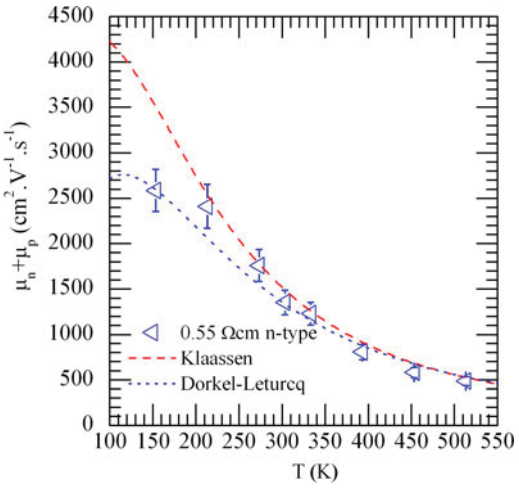

Fig. 6. Temperature dependence of the mobility sum in a 0.55 Ω·cm n-type silicon wafer. The lines represent the models of Dorkel–Leturcq and Klaassen.

C. Measuring the Influence of Temperature

An important application of this method is to study the impact of temperature on the carrier mobility sum. Using a temperature-controlled inductive coil photoconductance device [13] one can obtain the simultaneous temperature and injection dependence of the mobility. Fig. 6 shows the temperature dependence of the mobility sum at an injection level of 5×10^{15} cm^{-3}. At low temperature (153 K), the lattice scattering is very low, leading to a high mobility sum of around 2500 cm^2·V^{-1}·s^{-1}. At very high temperature (513 K), lattice scattering contributes to a drastic reduction of the mobility sum with an overall mobility of around 485 cm^2·V^{-1}·s^{-1}.

It is interesting to compare the temperature dependence of the mobility sum with mobility models at an injection level of 5×10^{15} cm^{-3}. The models of Klaassen and Dorkel–Leturcq are used as a comparison, since the model of Dannhauser does not include temperature dependence. Both Klaassen's and Dorkel–Leturcq's models are in relatively good agreement with the

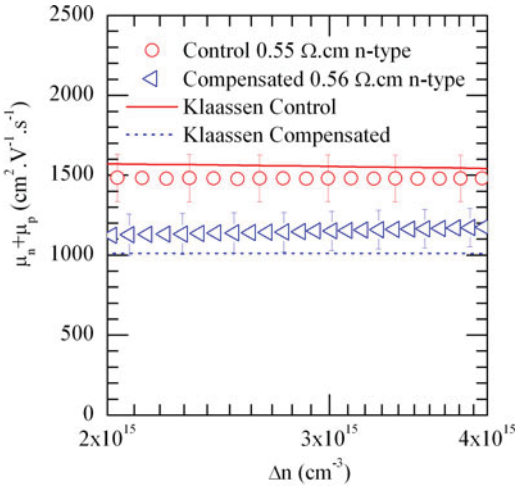

Fig. 7. Measured injection dependence of the mobility sum in 0.55 Ω·cm non-compensated and a 0.56 Ω·cm compensated silicon sample. The line represents the model of Klaassen.

experimental data at high temperature. For low temperatures, Klaassen's model seems to overestimate the mobility sum. Discrepancies between Klaassen's model and experimental data have been observed before at low (<200 K) or high (>400 K) temperatures [20]. However, the validity of Klaassen's model when both injection and temperature vary has not been assessed before.

D. Measuring the Influence of Compensation

Another important application of this method is to measure the impact of dopant compensation on the carrier mobility sum. Compensation doping has been found to be an efficient way to control ingot resistivity when using solar-grade silicon feedstocks [21]–[23]. Carrier recombination, which is being driven by the net doping rather than the sum of the dopant concentrations, can be improved by compensation [24]. However, the mobility is driven by the sum of the dopant concentrations rather than the net doping [25]. At similar resistivity, a significant reduction in mobility has been observed in compensated silicon [4]–[6]. Fig. 7 shows the mobility sum reduction due to compensation in two 0.55–0.56 Ω·cm n-type silicon samples, one of which was noncompensated ($N_D = 5 \times 10^{15}$ cm^{-3}), and the other compensated ($N_D = 5.3 \times 10^{16}$ cm^{-3}, $N_A = 5.0 \times 10^{16}$ cm^{-3}). Even though both samples have similar resistivities, the compensated sample has more ionized impurities, and, hence, lower mobility.

V. Conclusion

We have demonstrated the potential of a novel contactless method to measure the mobility sum in silicon wafers, based on combining transient and quasistatic photoconductance measurements. To be accurate, this method must be used in combination with a spectrophotometer in order to measure the optical properties of the sample used. This method is valid at medium injection where the lifetime and the photoconductance signal/noise ratio both remain high. We have shown that this method can measure the impact of dopant density, compensation, injection level, and temperature on the mobility sum. It is limited to samples with relatively high effective lifetime and thus requires surface passivation to ensure uniform carrier profiles throughout the sample thickness. However, through the use of an infrared LED array, for example, this technique could measure samples with lower lifetime. For the first time, we have measured the mobility sum reduction due to temperature and compensation.

Acknowledgment

The authors are grateful to B. Lim and J. Schmidt of the Institut für Solarenergieforschung Hameln/Emmerthal, for providing the compensated n-type sample, and to B. Geerligs of Energy Research Centre of the Netherlands and R. Sinton and J. Swirhun of Sinton Instruments, for helpful discussions in developing the technique.

References

[1] F. Dannhäuser, "Die abhängigkeit der trägerbeweglichkeit in silizium von der konzentration der freien ladungsträger–I," *Solid-State Electron.*, vol. 15, pp. 1371–1375, 1972.

[2] J. Krausse, "Die abhängigkeit der trägerbeweglichkeit in silizium von der konzentration der freien ladungsträger–II," *Solid-State Electron.*, vol. 15, pp. 1377–1381, 1972.

[3] L. Elstner, "Die Temperaturabhangigkeit der Defektelektronenbeweglichkeit in Siliziumkristallen," *Phys. Status Solidi B*, vol. 17, pp. 139–150, 1966.

[4] F. E. Rougieux, D. Macdonald, A. Cuevas, S. Ruffell, J. Schmidt, B. Lim, and A. P. Knights, "Electron and hole mobility reduction and Hall factor in phosphorus-compensated p-type silicon," *J. Appl. Phys.*, vol. 108, pp. 013706-1–013706-5, 2010.

[5] B. Lim, M. Wolf, and J. Schmidt, "Carrier mobilities in multicrystalline silicon wafers made from UMG-Si," *Phys. Status Solidi C*, vol. 235, pp. 835–838, 2011.

[6] J. Veirman, S. Dubois, N. Enjalbert, J.-P. Garandet, and M. Lemiti, "Electronic properties of highly-doped and compensated solar-grade silicon wafers and solar cells," *J. Appl. Phys.*, vol. 109, pp. 103711-1–103711-10, 2011.

[7] D. H. Neuhaus, P. P. Altermatt, A. B. Sproul, R. A. Sinton, A. Schenk, A. Wang, and A. G. Aberle, "Method for measuring majority and minority carrier mobility in solar cells," in *Proc. 17th Eur. Photovoltaic Solar Energy Conf.*, 2001, pp. 242–245.

[8] H. Nagel, C. Berge, and A. G. Aberle, "Generalized analysis of quasi-steady-state and quasi-transient measurements of carrier lifetimes in semiconductors," *J. Appl. Phys.*, vol. 86, pp. 6218–6221, 1999.

[9] A. Cuevas and R. A. Sinton, "Prediction of the open-circuit voltage of solar cells from the steady-state photoconductance," *Prog. Photovoltaics: Res. Appl.*, vol. 5, pp. 79–90, 1997.

[10] R. A. Sinton and T. Trupke, "Limitations on dynamic excess carrier lifetime calibration methods," *Prog. Photovoltaics: Res. Appl.*, 2011, to be published. Available: http://onlinelibrary.wiley.com/doi/10.1002/pip.1119/abstract.

[11] J. Tan, D. Macdonald, F. Rougieux, and A. Cuevas, "Accurate measurement of the formation rate of iron-boron pairs in silicon," *Semicond. Sci. Technol.*, vol. 26, pp. 055019-1–055019-5, 2011.

[12] R. A. Sinton and A. Cuevas, "Contactless determination of current–voltage characteristics and minority-carrier lifetimes in semiconductors from quasi-steady-state photoconductance data," *Appl. Phys. Lett.*, vol. 69, pp. 2510–2512, 1996.

[13] B. B. Paudyal, K. R. McIntosh, D. H. Macdonald, B. S. Richards, and R. A. Sinton, "The implementation of temperature control to an inductive-coil photoconductance instrument for the range of 0–230 °C," *Prog. Photovoltaics: Res. Appl.*, vol. 16, pp. 609–613, 2008.

[14] T. Trupke and R. A. Bardos, "Self-consistent determination of the generation rate from photoconductance measurements," *Appl. Phys. Lett.*, vol. 85, pp. 3611–3613, 2004.

[15] J. Brody, A. Rohatgi, and A. Ristow, "Guidelines for more accurate determination and interpretation of effective lifetime from measured

quasi-steady-state photoconductance," presented at the 11th Workshop Crystalline Silicon Solar Cell Mater. Processes, Estes Park, CO, Aug. 19–22, 2001.

[16] T. Roth, T. Rosenits, W. Warta, and S. W. Glunz, "Photoconductance-based excess carrier lifetime measurements on unpassivated silicon samples," in *Proc. 24th Eur. Photovoltaic Solar Energy Conf.*, Hamburg, Germany, 2009, pp. 2004–2007.

[17] D. B. M. Klaassen, "A unified mobility model for device simulation—I. Model equations and concentration dependence," *Solid-State Electron.*, vol. 35, pp. 953–959, 1992.

[18] D. B. M. Klaassen, "A unified mobility model for device simulation—II. Temperature dependence of carrier mobility and lifetime," *Solid-State Electron.*, vol. 35, pp. 961–967, 1992.

[19] J. M. Dorkel and P. Leturcq, "Carrier mobilities in silicon semi-empirically related to temperature, doping and injection level," *Solid-State Electron.*, vol. 24, pp. 821–825, 1981.

[20] S. Reggiani, M. Valdinoci, L. Colalongo, M. Rudan, G. Baccarani, A. D. Stricker, F. Illien, N. Felber, W. Fichtner, and L. Zullino, "Electron and hole mobility in silicon at large operating temperatures—Part I: Bulk mobility," *IEEE Trans. Electron Devices*, vol. 49, no. 3, pp. 490–499, Mar. 2002.

[21] J. Kraiem, R. Einhaus, and H. Lauvray, "Doping engineering as a method to increase the performance of purified MG silicon during ingot crystallisation," in *Proc. 34th IEEE Photovoltaic Spec. Conf.*, Philadelphia, PA, 2009, pp. 001327–001330.

[22] D. Macdonald, A. Cuevas, "Carrier recombination and transport in compensated silicon, and prospects for "compensation engineering,"' presented at the 19th Workshop Crystalline Silicon Solar Cells Modules: Mater. Processes, Vail, CO, 2009.

[23] M. Forster, E. Fourmond, R. Einhaus, H. Lauvray, J. Kraiem, and M. Lemiti, "Ga co-doping in Cz-grown silicon ingots to overcome limitations of B and P compensated silicon feedstock for PV applications," *Phys. Status Solidi C*, vol. 8, pp. 678–681, 2011.

[24] D. Macdonald and A. Cuevas, "Recombination in compensated crystalline silicon for solar cells," *J. Appl. Phys.*, vol. 109, pp. 043704-1–043704-8, 2011.

[25] F. E. Rougieux, D. Macdonald, and A. Cuevas, "Transport properties of p-type compensated silicon at room temperature," *Prog. Photovoltaics: Res. Appl.*, vol. 19, pp. 787–793, 2011.

Authors' photographs and biographies not available at the time of publication.